LA-UR-16-20090

Title: Energetic Light Fragment Production Capability in MCNP6

Author(s): Kerby, Leslie Marie
Mashnik, Stepan Georgievich
Gudima, Konstantin K.
Sierk, Arnold John
Bull, Jeffrey S.
James, Michael R.

Intended for: ANS 2016 Annual Meeting, 2016-06-12/2016-06-16 (New Orleans, Louisiana, United States)

Issued: 2016-01-08

Energetic Light Fragment Production Capability in MCNP6

Leslie M. Kerby,[*,†] Stepan G. Mashnik,[†] Konstantin K. Gudima,[‡] Arnold J. Sierk,[†] Jeffrey S. Bull,[†] and Michael R. James[†]

[*]*Idaho State University, Pocatello, ID*
[†]*Los Alamos National Laboratory, Los Alamos, NM*
[‡]*Institute of Applied Physics, Academy of Science of Moldova, Chişinău, Moldova*
kerblesl@isu.edu

INTRODUCTION

The Monte Carlo Methods, Codes, and Applications group within the Computational Physics Division at Los Alamos National Laboratory has led the development of the transport code MCNP6 (Monte Carlo N-Particle transport code, version 6) [1]. MCNP6 is a general-purpose, continuous-energy, generalized-geometry, time-dependent, Monte-Carlo radiation-transport code designed to track many particle types over broad ranges of energies. It is used around the world in applications ranging from radiation protection and dosimetry, nuclear-reactor design, nuclear criticality safety, detector design and analysis, decontamination and decommissioning, accelerator applications, medical physics, space research, and beyond. At lower energies, the code uses tables of evaluated nuclear data, while for higher energies (> 150 MeV), MCNP6 uses the cascade-exciton model, version 03.03 (CEM03.03) [2, 3], and the Los Alamos quark-gluon string model, version 03.03 (LAQGSM03.03) [3, 4] to model nuclear reactions.

Emission of energetic heavy clusters heavier than ^{4}He from nuclear reactions play a critical role in several applications, including electronics performance in space, human radiation dosages in space or other extreme radiation environments, proton- and hadron-therapy in medical physics, accelerator and shielding applications, and more. None of the available models are able to accurately predict emission of light fragments (LF) from arbitrary reactions. The CEM and LAQGSM event generators in MCNP6 describe quite well the spectra of fragments with sizes up to ^{4}He across a broad range of target masses and incident energies (up to $\sim$ 5 GeV for CEM and up to $\sim$ 1 TeV/A for LAQGSM). However, they do not predict the high-energy tails of LF spectra heavier than ^{4}He well. Most LF with energies above several tens of MeV are emitted during the precompound stage of a reaction. The 03.03 versions of CEM and LAQGSM do not account for precompound emission of LF larger than ^{4}He.

The goal of this research is to enable MCNP6 to produce high-energy light fragments. These energetic LF may be emitted by our models through three processes: Fermi breakup, preequilibrium, and coalescence. We explore the emission of light fragments through each of these mechanisms and demonstrate an improved agreement with experimental data achieved by extending precompound models to include emission of fragments heavier than ^{4}He.

FERMI BREAKUP

The Fermi breakup model is used in CEM and LAQGSM for residual nuclei with atomic mass number $A \leq 12$, making it particularly important for reactions with light target nuclei.

De-excitation of light nuclei with $A \leq A_{\text{Fermi}}$ remaining after the Intra-Nuclear Cascade is described in CEM and LAQGSM only with the Fermi breakup model, where A_{Fermi} is a 'cut-off value' fixed in the models. The value of A_{Fermi} is a model parameter, not a physical characteristic of nuclear reactions. Actually, the initial version of the Fermi breakup model incorporated into CEM and LAQGSM used $A \leq A_{\text{Fermi}} = 16$, just as $A_{\text{Fermi}} = 16$ is used currently in GEANT4 [5] and in SHIELD-HIT [6]. But that initial version of the Fermi breakup model had some problems and code crashes in some cases. To avoid unphysical results and code crashes, we chose the expedient of using $A_{\text{Fermi}} = 12$ in both CEM and LAQGSM. Later, the problems in the Fermi breakup model were fixed, and we studied how the value of A_{Fermi} affected the final results of those codes.

We found that the performance of MCNP6, CEM, and LAQGSM in simulating fragmentation reactions at intermediate energies for targets with $A < 13$ provide reasonably good predictions for all reactions tested, although a fine-tuning of the A_{Fermi} cut-off parameter in the Fermi breakup model might provide a better description of some experimental data. However, in some cases $A_{Fermi} = 12$ provided the best agreement with experimental data, and so we did not find sufficient evidence to change the Fermi cut-off value in MCNP6, CEM, and LAQGSM at that time. See Ref. [7] for complete results.

PREEQUILIBRIUM

The preequilibrium interaction stage of nuclear reactions is considered by the current CEM and LAQGSM in the framework of the latest version of the modified exciton model (MEM) [8, 9]. At the preequilibrium stage of a reaction, CEM03.03 and LAQGSM03.03 take into account all possible nuclear transitions changing the number of excitons n with $\Delta_n = +2$, -2, and 0, as well as all possible multiple subsequent emissions of n, p, d, t, ^{3}He, and ^{4}He. The corresponding system of master equations describing the behavior of a nucleus at the preequilibrium stage is solved by the Monte-Carlo technique. Improvements to the preequilibrium stage were three-fold: extension of preequilibrium to include LF emission up to ^{28}Mg, adoption of the NASA reaction cross section as the inverse cross section, and the creation of a new model for the condensation probability γ_j.

Preequilibrium extension

CEM03.03 does not have the capability to output cross sections for fragments larger than ^{4}He. Therefore, one of the first things done was to add this capability. We also created the capability to output by isotope, Z number, or mass number.

Extending the MEM to produce 66 fragment types, up to ^{28}Mg, involves extending the calculation of emission widths (Eq. (1)) to all 66 fragment types. The emission width Γ_j, (or probability of emitting particle fragment j), is estimated as

$$\Gamma_j(p, h, E) = \int_{V_j^c}^{E-B_j} \lambda_j(p, h, E, T) dT, \qquad (1)$$

where the partial transmission probabilities, λ_j, are equal to

$$\lambda_j(p, h, E, T) = \gamma_j \frac{2s_j + 1}{\pi^2 \hbar^3} \mu_j \Re(p, h) \frac{\omega(p_j, 0, T + B_j)}{g_j} \\ \times \frac{\omega(p - p_j, h, E - B_j - T)}{\omega(p, h, E)} T \sigma_j^{inv}(T), \qquad (2)$$

for complex particles and fragments. This extension therefore entails calculating Coulomb barriers, binding energies, reduced masses, inverse cross sections, and condensation probabilities for all 66 fragment types.

The extended MEM provides dramatically improved ability to describe light-fragment production at intermediate to high energies across most reactions tested, while maintaining good results for fragments $\leq {}^4$He.

Inverse Cross Sections

Total-reaction-cross-section models have a significant impact on the predictions and accuracy of spallation and transport codes. For example, CEM uses total reaction cross sections as *inverse* cross sections, σ_j^{inv}, to calculate the probabilities of emission of possible nucleons and fragments.

The inverse cross sections in CEM03.03 are taken from the Dostrovsky et al. model [10]. Its general form is:

$$\sigma_{Dost.} = \pi r_0^2 A^{2/3} \alpha_j (1 - \frac{V_j}{T}). \qquad (3)$$

The Dostrovsky model was not intended for use above about 50 MeV/nucleon, and is not very suitable for emission of fragments heavier than ^{4}He. Better total-reaction-cross-section models are available today. We compared results from several total reaction cross section models and determined the NASA (or Tripathi et al.) model [11] provided the best general agreement with experimental data. As shown in Eq. (4), the NASA cross section attempts to simulate several quantum-mechanical effects, such as the optical potential for neutrons (with the parameter X_m) and collective effects like Pauli blocking (through the quantity δ_T).

$$\sigma_{NASA} = \pi r_0^2 (A_P^{1/3} + A_T^{1/3} + \delta_T)^2 (1 - R_c \frac{B_T}{T_{cm}}) X_m. \qquad (4)$$

Results of implementing the NASA inverse-cross-section model into the extended MEM show improved agreement with experimental data. See Ref. [12] for details.

Condensation probability γ_j

The condensation probability, γ_j, represents the probability that p_j excited nucleons (excitons) will condense to form a complex particle of type j in the excited residual nucleus. We explore the formulation of a new model for γ_j, one which is energy-dependent, and which provides improved fits to experimental fragment spectra.

The condensation probability γ_j could be calculated from first principles, but such a calculation is not feasible. γ_j is, therefore, estimated as the overlap integral of the wave function of independent nucleons with that of the complex particle (see details in [2]), as shown in Eq. (5).

$$\gamma_j \approx p_j^3 (\frac{p_j}{A})^{p_j - 1}. \qquad (5)$$

Eq. (5) is a rather crude estimate. In CEM we approximate γ_j by multiplying the estimate provided by Eq. (5) by empirical coefficients F_j. Values of F_j for d, t, ^{3}He, and ^{4}He need to be re-fit after the upgrades to the inverse-cross-section and coalescence models, and new values of F_j need to be obtained for heavy clusters up to ^{28}Mg.

In analyzing the fitted F_j data set we created mathematical models for both the fragment-specific equations for F_j and a generalized F_j model. The general F_j model is:

$$F_j(T_0, A_j, Z_j, A_t) = \left[7800(2.5)^{A_j} e^{-T_0/20} + \frac{2(4)^\tau}{T_0^{0.2\tau} + 100} \right] \\ \times e^{-\frac{300 - A_t}{100}}, \qquad (6) \\ \tau = A_j - (Z_j - 3).$$

For the fragment-specific F_j, discussion of the physical meaning of the model, and results, see Ref. [13].

COALESCENCE

CEM03.03 is capable of producing light fragments up to ^{4}He in its coalescence model. We extend the coalescence model to be able to produce up to ^{7}Be in CEM and up to ^{12}C in LAQGSM.

When the cascade stage of a reaction is completed, CEM uses the coalescence model to create high-energy d, t, ^{3}He, and ^{4}He fragments by final-state interactions among emitted cascade nucleons outside of the target nucleus. The magnitude of the momentum, p, of each cascade nucleon is calculated relativistically from its kinetic energy, T. We assume that all the cascade nucleons having differences in their momenta smaller than p_c and with the correct isotopic content form an appropriate composite particle.

The coalescence model first checks all nucleons to form 2-nucleon pairs, their momenta permitting. It then takes these 2-nucleon pairs and the single nucleons left and forms ^{4}He, ^{3}He, and/or tritium, their momenta permitting. The extended coalescence model further takes these two-nucleon pairs, tritium, ^{3}He, and ^{4}He to see if they can coalesce to form heavier clusters: ^{6}He, ^{6}Li, ^{7}Li or ^{7}Be.

All coalesced nucleons are removed from the distributions of nucleons so that atomic and mass numbers are conserved.

Results show significant improvement in the production of heavy clusters across the energy range. However, too many alpha particles were lost (coalesced into heavy clusters); so $p_c(^4$He$)$ was increased to compensate. See Refs. [14] and [15]

for details. The new values for p_c for the extended coalescence model are:

$$p_c(d) = 90 \text{ MeV/c} ;$$
$$p_c(t) = p_c(^3\text{He}) = 108 \text{ MeV/c} ;$$
$$p_c(^4\text{He}) = 130 \text{ MeV/c} ;$$
$$p_c(LF) = 175 \text{ MeV/c} .$$
(7)

For $300 \text{ MeV} < T < 1000 \text{ MeV}$ they are:

$$p_c(d) = 150 \text{ MeV/c} ;$$
$$p_c(t) = p_c(^3\text{He}) = 175 \text{ MeV/c} ;$$
$$p_c(^4\text{He}) = 205 \text{ MeV/c} ;$$
$$p_c(LF) = 250 \text{ MeV/c} .$$
(8)

MCNP6 IMPLEMENTATION

The culmination of this work is the implementation of CEM with these heavy-cluster upgrades, which we call CEM03.03F, into MCNP6.

The GENXS option allows for various cross sections to be tallied in MCNP6. Previously, production cross sections were only available for fragments up to ^{4}He. Thus, a necessary first step in implementing the improved CEM03.03F into MCNP6 involves extending the ability to output production cross sections to heavy clusters. This GENXS upgrade accomplishes this and includes the ability to tally and output double differential cross sections, angle-integrated or energy-integrated cross sections, as well as the total production cross section, for any heavy ion with valid ZAID. For details see Ref. [16].

CEM03.03F was implemented into a working version of MCNP6, which we call MCNP6-F. Two of the upgrades are always implemented: the upgraded NASA-Kalbach inverse cross sections in the preequilibruim stage, and the new energy-dependent γ_j model. The other two upgrades (extension of preequilibrium emission to ^{28}Mg, and the extension of the coalescence model to ^{7}Be), both of which increase computation time, may be turned off if desired. A variable, called npreqtyp, was created to specify the number of preequilibrium particles considered for emission. It is now the twelfth option on the LCA card of the MCNP6 input file. Its maximum (and default) value is 66, similar to the nevtype variable used for the evaporation stage. See Ref. [17] for a list of the 66 particles considered in the preequilibrium stage. In the old model, 6 preequilibrium particles were considered, and therefore a value of npreqtyp=6 turns off both the preequilibrium and coalescence extensions. The extended coalescence model is implemented for values of npreqtyp>6. MCNP6-F also includes the GENXS extension.

Basic testing and verification of MCNP6-F has been completed with the results being presented below. In addition, MPI testing has been completed. Upon further testing, we anticipate these heavy-ion upgrades and the GENXS extension will be included in the next release of MCNP6.

Results

Double differential cross section spectra for several reactions are plotted in this section. Fig. 1 shows the results
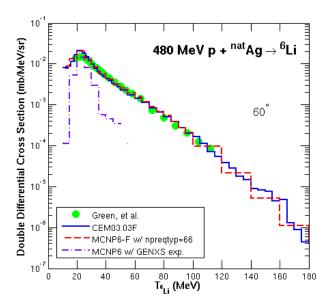

Fig. 1. Comparison of experimental data for 480 MeV p + ^{nat}Ag $\rightarrow$ ^{6}Li at 60°, measured by Green, et al. [18] (green circles) to calculated results from CEM03.03F (blue solid lines), MCNP6-F with npreqtyp=66 (red dashed lines), and MCNP6 with the GENXS extension only (purple dash-dotted lines).

for 480 MeV p + ^{nat}Ag $\rightarrow$ ^{6}Li at 60°, compared to experimental data measured by Green, et al. [18]. MCNP6 with the GENXS extension only does not contain any of the four light-fragment upgrades discussed in this work. MCNP6-F produces significantly improved results and matches the data reasonably well.

Fig. 2 displays the results for 200 MeV p + ^{197}Au $\rightarrow$ ^{7}Be at 45°, compared to experimental data by Machner, et al. [19]. This figure shows not only dramatically improved heavy-cluster production by MCNP6-F at high energies, but also improved production at relatively low energies around the preequilibrium peak. We believe this is due to the heavy target (gold) and therefore an increased ability to produce these low-energy heavy clusters from both the extended coalescence model and the extended preequilibrium model.

Across the reactions we tested we found that the new MCNP6-F, in general, gives improved results compared to the unmodified MCNP6, most especially for heavy-cluster spectra. Further details and more results can be found in Ref. [17].

The goal of producing energetic light fragments in MCNP6 has been accomplished by implementing several heavy-cluster upgrades as outlined in this paper.
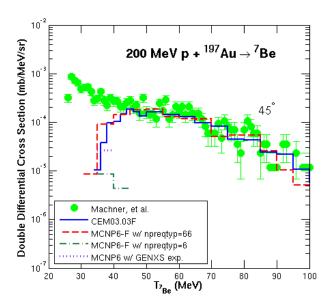
Fig. 2. Comparison of experimental data for 200 MeV p + $^{197}Au \rightarrow {}^{7}Be$ at 45°, measured by Machner, et al. [19] (green circles) to calculations from CEM03.03F (blue solid lines), MCNP6-F with npreqtyp=66 (red dashed lines), MCNP6-F with npreqtyp=6 (green dash-dotted lines), and MCNP6 with the GENXS extension only (purple dotted lines).

REFERENCES

1. T. GOORLEY, et al., "Initial MCNP6 Release Overview, MCNP6 version 0.1," *Nuclear Technology*, **180**, 298–315 (2012).

2. K. GUDIMA, S. MASHNIK, and V. TONEEV, "Cascade-Exciton Model of Nuclear Reactions," *Nuclear Physics A*, **401**, 329–361 (1983).

3. S. MASHNIK, K. GUDIMA, R. PRAEL, A. SIERK, M. BAZNAT, and N. MOKHOV, "CEM03.03 and LAQGSM03.03 Event Generators for the MCNP6, MCNPX, and MARS15 Transport Codes," Joint ICTP-IAEA Advanced Workshop on Model Codes for Spallation Reactions. Trieste, Italy (February 2008), LANL Report LA-UR-08-2931, arXiv:0812.1820.

4. K. GUDIMA, S. MASHNIK, and A. SIERK, "User Manual for the code LAQGSM," (2001), LANL Report LA-UR-01-6804; http://lib-www.lanl.gov/lapubs/00818645.pdf.

5. I. PSHENICHNOV, A. BOTVINA, I. MISHUSTIN, and W. GRAINER, "Nuclear Fragmentation Reactions in Extended Media Studied with GEANT4 Toolkit," *Nuclear Instruments and Methods in Physics Research B*, **268**, 604 (2010).

6. M. HULTQVIST, M. LAZZERONI, A. BOTVINA, I. GUDOWSKA, N. SOBOLEVSKY, and A. BRAHME, "Evaluation of Nuclear Reaction Cross-Sections and Fragment Yields in Carbon Beams Using the SHIELD-HIT Monte Carlo Code. Comparison with Experiments," *Physics in Medicine & Biology*, **57**, 4369 (2012).

7. S. MASHNIK and L. KERBY, "MCNP6 Fragmentation of Light Nuclei at Intermediate Energies," *Nuclear Instruments and Methods in Physics Research A*, **764**, 59 (2014), arXiv:1404.7820.

8. K. GUDIMA, G. OSOSKOV, and V. TONEEV, "Model for Pre-Equilibrium Decay of Excited Nuclei," *Yadernaya Fizika*, **21** (1975), [Soviet Journal of Nuclear Physics 21 (1975) 139-143].

9. S. MASHNIK and V. TONEEV, "MODEX–the Program for Calculation of the Energy Spectra of Particles Emitted in the Reactions of Pre-Equilibrium and Equilibrium Statstical Decays," *JINR Communication*, **P4-8417** (1974).

10. I. DOSTROVSKY, Z. FRAENKEL, and G. FRIEDLANDER, "Monte Carlo Calculations of Nuclear Evaporation Processes. III. Applications to Low-Energy Reactions," *Physical Review*, **116**, 683 (1959).

11. R. TRIPATHI, F. CUCINOTTA, and J. WILSON, "Accurate Universal Parameterization of Absorption Cross Sections," *Nuclear Instruments and Methods in Physics Research B*, **117**, 347 (1996).

12. L. KERBY and S. MASHNIK, "Total Reaction Cross Sections in CEM and MCNP6 at Intermediate Energies," *Nuclear Instruments and Methods B*, **356-357**, 135 (2015).

13. L. KERBY, "An Energy-Dependent Numerical Model for the Condensation Probability, γ_j," LANL Report, LA-UR-15-26648 (2015).

14. K. GUDIMA, S. MASHNIK, and L. KERBY, "Fragmentation of Light Nuclei at Intermediate Energies Simulated with MCNP6," LANL Report, LA-UR-15-27417, presented at the Fifth International Conference on Nuclear Fragmentation From Basic Research to Applications (NUFRA2015), 4 – 11 October 2015, Kemer (Antalya), Turkey (2015).

15. L. KERBY and S. MASHNIK, "Production of Heavy Clusters with an Expanded Coalescence Model in CEM," *Transactions of the American Nuclear Society*, **112**, 577 (2015).

16. L. KERBY, S. MASHNIK, and J. BULL, "MCNP6 GENXS Option Expansion to Include Fragment Spectra of Heavy Ions," LANL Report, LA-UR-15-27858 (2015), summary accepted for presentation at PHYSOR 2016, Sun Valley, Idaho, USA, May 1-5, 2016.

17. L. KERBY, S. MASHNIK, K. GUDIMA, A. SIERK, J. BULL, and M. JAMES, "Production of Energetic Heavy Clusters in CEM and MCNP6," LANL Report, LA-UR-15-29524 (2015).

18. R. GREEN, R. KORTELING, and K. JACKSON, "Inclusive Production of Isotopically Resolved Li Through Mg Fragments by 480 MeV p+Ag Reactions," *Physical Review C*, **29**, 1806–1824 (1984).

19. H. MACHNER, et al., "Isotopic production cross sections in proton-nucleus collisions at 200 MeV," *Physical Review C*, **73**, 044606 (2006).